



# Diagnostic test of dynamic computed tomography in early gastrointestinal lymphoma and precancerous lesions

Jingcong Chen, Yu Zhong, Xiangling Zeng, Chunyu Huang, Bowen Lan

Department of Radiology, Huizhou Municipal Central People's Hospital, Huizhou, China

**Contributions:** (I) Conception and design: J Chen, Y Zhong; (II) Administrative support: X Zeng; (III) Provision of study materials or patients: J Chen, C Huang, B Lan; (IV) Collection and assembly of data: J Chen, Y Zhong, X Zeng, B Lan; (V) Data analysis and interpretation: J Chen, C Huang, B Lan; (VI) Manuscript writing: All authors; (VII) Final approval of manuscript: All authors.

**Correspondence to:** Jingcong Chen. Department of Radiology, Huizhou Municipal Central People's Hospital, Huizhou 516001, China.

Email: chanjingcong2011@163.com.

**Background:** In recent years, with the development of imaging technology, the accurate diagnosis of precancerous lesions of digestive system and early lymphoma has attracted wide attention in the medical field.

**Methods:** In this study, 82 patients with gastrointestinal diseases, including 32 patients with early gastrointestinal lymphoma and 50 patients with gastrointestinal precancerous lesions, underwent dynamic contrast-enhanced computed tomography (CT) scanning. The difference ( $\delta_1$ ,  $\delta_2$ ) and ratio ( $Q_1$ ,  $Q_2$ ) of density between arterial phase, portal phase and plain scan were measured and compared, and the receiver operating characteristic (ROC) curve of the subjects was drawn.

**Results:** The results showed no statistically significant differences in the general condition of patients or a difference for the results of the arterial phase  $\delta_1$  and  $Q_1$  between the two groups ( $P>0.05$ ). However, the portal venous phase  $\delta_2$  and  $Q_2$  in the early lymphoma group and in precancerous lesion group were  $29.50\pm 6.05$ ,  $41.55\pm 10.10$  Hounsfield units (HU), and  $1.70\pm 0.05$ ,  $2.06\pm 0.31$ , respectively. The area under the ROC curve (AUC) values for  $\delta_2$  and  $Q_2$  to identify the two diseases were 0.755 and 0.878, respectively. When  $\delta_2$  and  $Q_2$  were 35.63 and 1.86 HU, the specificity was 89.60% and 67.50%, and sensitivity was 89.60% and 64.90%, respectively. When the two indexes,  $\delta_2$  and  $Q_2$ , were combined, the specificity and sensitivity of diagnosis were 98.99% and 56.80%, respectively.

**Conclusions:** Dynamic contrast-enhanced CT can effectively distinguish early gastrointestinal lymphoma from precancerous lesions and improve the diagnostic accuracy.

**Keywords:** Dynamic enhanced computed tomography (dynamic enhanced CT); early gastrointestinal lymphoma; precancerous lesions; receiver operating characteristic curve (ROC curve)

Submitted Apr 02, 2022. Accepted for publication Jun 09, 2022.

doi: 10.21037/tcr-22-1085

**View this article at:** <https://dx.doi.org/10.21037/tcr-22-1085>

## Introduction

There are two types of malignant lymphoma: malignant tumors of the lymph nodes and malignant tumors of tissues beyond the lymph nodes. It is a malignant tumor mainly of lymphocytes in the body (1). Lymphoma can occur at any age, but mostly in middle and young age and there are more male patients than female patients (incidence ratio  $\approx 3:1$ ) (2). In China, malignant lymphoma ranks 8th among new cases of all tumors and 10th among new cases of female tumors, with

an incidence of about 6–7 cases per 100,000 (3). In clinical pathology, lymphoma is generally divided into Hodgkin's lymphoma and non-Hodgkin's lymphoma (NHL), the latter being one of the cancers with the fastest increasing incidence, accounting for >90%. To date, the etiology and pathogenesis of lymphoma are not clear, and most researchers consider that it is related to psychological stress, blood transfusion, viral infection, immune suppression caused by the treatment of other diseases such as organ transplantation and industrial

environmental pollution (4,5).

Gastrointestinal lymphoma originates from the gastrointestinal tract, and includes gastric and small intestine lymphoma and immune deficiency-associated lymphoma. It is relatively rare; most cases are NHL, and B-cell lymphoma is common (6). Among gastrointestinal lymphoma, the highest incidence rate is gastric lymphoma, followed by small intestinal lymphoma and colon lymphoma. The specific pathogenesis is unclear at present, but some experts speculate that it is related to interaction of internal and external factors that disturbs homeostasis, resulting in abnormal proliferation and differentiation of lymphocytes (7). Several findings have led to this speculation. (I) It has been associated with bacterial infections such as *Helicobacter pylori* (HP) (8). (II) Chromosomal aberrations (structural aberration or chromosome number abnormality such as deletion, translocation, and insertion) are identified in >90% of patients with lymphoma (9). (III) The incidence of gastrointestinal lymphoma is increased by the long-term effects of physical and chemical factors or high doses of radiation (10). (IV) Retroviruses can infect T lymphocytes in human body, and the acquired immune deficiency syndrome (AIDS) virus is a retrovirus. About 5–10% of AIDS patients develop lymphoma, especially of the small intestine (11). (V) Primary lymphoma of the small intestine is caused by many diseases, as well as immune dysfunction (12).

It is well known that the occurrence and development of malignant tumors is a long and complex process from normal epithelial cells to simple hyperplasia to atypical hyperplasia to carcinoma in situ to invasive cancer, precipitated by carcinogenic factors. The scientific consensus is that precancerous lesions begin with atypical hyperplasia (13), but the occurrence and development of cancer is not inevitable. Nevertheless, the vast majority of cancers have obvious precancerous lesions. Thus, identifying precancerous lesions at the early stage of the disease is a very valuable opportunity for early diagnosis and treatment (14,15).

With medical endoscopy becoming more commonly performed in recent years, precancerous lesions of the digestive system and early-stage lymphoma have attracted the attention of the medical community (16). If accurate early diagnosis can be made and the most effective early treatment is implemented, the survival rate of patients will be remarkably increased and their quality of life improved. Complete cure can be achieved (17).

Dynamic computed tomography (CT) scan is a method of scanning after intravenous injection of water-soluble

contrast agent, which can improve the density difference between the lesion and adjacent tissues to reflect the lesion and improve the display rate of the lesion. It has been widely used in recent years, especially in the differential diagnosis of lymphoma, which has obvious advantages over conventional imaging (18). Dynamic enhanced CT is used by clinicians to make a preliminary judgment of pathological changes and then effective treatment measures are implemented (19,20).

In this study, we used dynamic enhanced CT to explore its diagnostic value in differentiating early gastrointestinal lymphoma from precancerous lesions, thus providing a theoretical basis for the differential diagnosis of these two diseases in clinical practice. We present the following article in accordance with the STARD reporting checklist (available at <https://tcr.amegroups.com/article/view/10.21037/tcr-22-1085/rc>).

## Methods

### General data

The study group comprised 82 patients with gastrointestinal lesions admitted to the Department of Gastroenterology of Huizhou Municipal Central People's Hospital from May 2018 to May 2021. The study was conducted in accordance with the Declaration of Helsinki (as revised in 2013). The study was approved by ethics board of Huizhou Municipal Central People's Hospital (No. kyll20210108) and informed consent was taken from all the patients. All patients complained of long-term abdominal discomfort.

The inclusion criteria were: age between 16 and 82 years; recurrent abdominal discomfort (abdominal pain, abdominal distention), hiccups, acid reflux, loss of appetite, body fatigue, and other symptoms; all relevant clinical data available; suspicious lesions found by routine gastroscopy, such as abnormal morphology on the surface of gastric mucosa or abnormal morphology of microvessels or even disappearance, clear lesions, mucosal congestion, swelling, granular appearance, and erosion, consistent with relevant diagnostic and treatment guidelines (21).

The exclusion criteria were: coagulation dysfunction; unable to tolerate the examination method; digestive tract obstruction or esophageal varices; respiratory tract infection within the past 3 months; serious dysfunction of heart, liver, spleen, kidney, lung, or other organs; pregnancy or lactation; history of radical treatment of HP infection or a history of gastric surgery; participation in other clinical trials simultaneously; history of taking nonsteroidal anti-

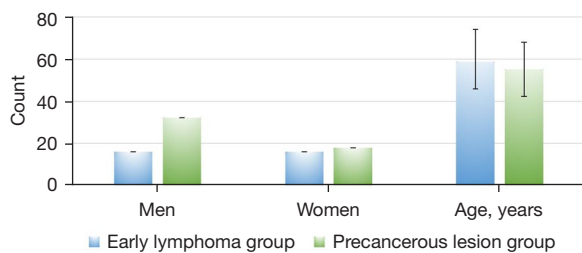


**Figure 1** Comparison of general data between the two groups revealed no statistically significant difference in age or sex ( $P>0.05$ ).

inflammatory drugs in the past 6 months; abnormal mental or cognitive function; advanced gastric cancer, gastric polyps, or gastric bleeding diagnosed by gastroscopy.

### CT scanning

All patients underwent CT examination by a 64-slice spiral CT scanner Lightspeed VCT (GE Company, Boston, USA). Patients were asked to fast for 4–6 h and drink 800–1,200 mL of water 45 min before the scan, as well as another 250 mL of water when entering the CT room. The patients lay supine during the scan. An ANT200200 CT double-cylinder high-pressure syringe (Antecedent Medical Co., Ltd., Shenzhen, China) was used to inject 85–110 mL of contrast agent (ioversol 320, iodine content 1 mL:320 mg I) through the median cubital vein at a flow rate of 2.0 mL/s. The scanning delay times were 30 and 50 s. Dynamic enhanced CT scanning was implemented in the arterial and portal vein phases, which required patients to hold their breath. The scanning range was from the upper diaphragm to the lower margin of both kidneys, with the following parameters: scanning layer thickness 5.0 mm, scanning layer spacing 5.0 mm, tube voltage 120 kV, and tube current 220 mA.

### CT imaging analysis

The final analysis of the CT images was performed by two experienced radiologists: a resident with 5 years of clinical experience, and an associate chief physician with 12 years of clinical experience. The size of the region of interest (ROI) in the center of the lesion was determined and measured in the uniform density of the lesion, about 8–22 mm<sup>2</sup>. Areas of necrosis and vascular structures were not outlined together. At the same time, the CT values of the plain scan, the arterial phase, and the portal venous phase areas of the ROI of each lesion were measured. The average value was

calculated from the results of the three measurements.

### Observation indexes

The following indexes were recorded: (I) comparison of the general data of the patients; (II) comparison of lesion sites between the two groups of patients; (III) comparison of thickness of the affected gastric wall between the two groups; (IV) comparison of the density difference of the arterial phase and plain scan CT ( $\delta 1$ ) and the density ratio of the arterial phase and plain scan CT ( $Q1$ ) between the two groups; (V) comparison of the density difference of the portal vein phase and plain scan CT ( $\delta 2$ ) and the density ratio of portal vein phase and plain scan CT ( $Q2$ ) between the two groups.

### Statistical analysis

SPSS 20.0 was used for statistical data analysis. Measurement data are expressed as mean  $\pm$  standard deviation and enumeration data are represented by number. The measurement data were in accordance with a normal distribution. Independent *t*-test was used to test the difference of parameter characteristics between the two groups of patients undergoing dynamic enhanced CT. Taking pathological diagnosis results as the gold standard, receiver operating characteristic (ROC) curve of different dynamic contrast-enhanced CT scanning parameters was drawn, the area under ROC curve (AUC) was calculated, and the maximum matching value of Youden Index (YI) was taken as the diagnosis threshold. The difference was statistically significant at  $P<0.05$ .

## Results

### General data of the patients

The 82 patients with gastrointestinal lesions were classified as early lymphoma ( $n=32$ ) and precancerous lesion ( $n=50$ ) groups based on the type of lesion. *Figures 1,2* respectively show the general data and CT images of the patients in the two groups after admission.

### Comparison of lesion sites and the affected gastric wall thickness in the two groups

The most commonly involved sites of early lymphoma were the gastric antrum and gastric body, whereas the most

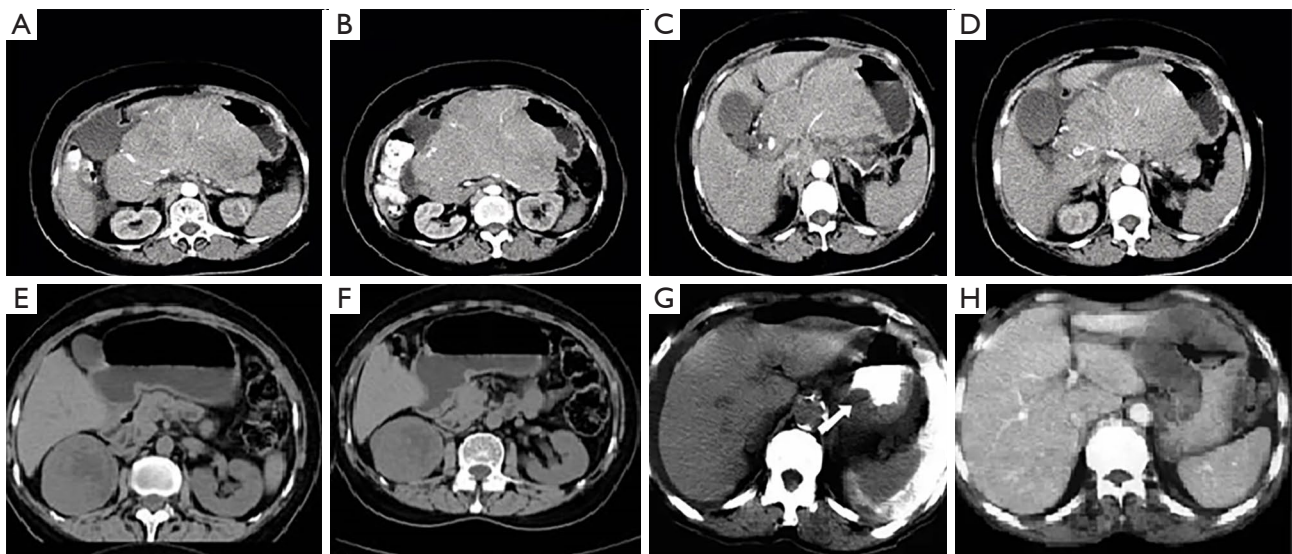


**Figure 2** Representative CT images of patients from the two groups. Plain CT images (A,B) and enhanced CT images (C,D) of early gastric lymphoma. Plain CT images (E,F) and enhanced CT images (G,H) of precancerous lesions (white arrow pointed to the lesion site). CT, computed tomography.

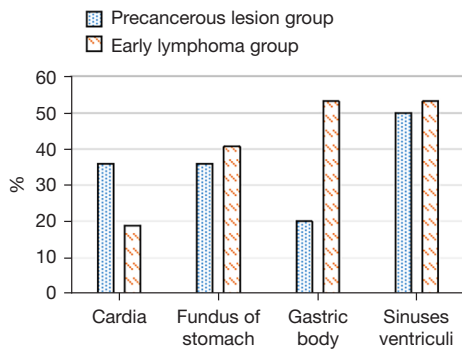


**Figure 3** Comparison of lesion sites between two groups.

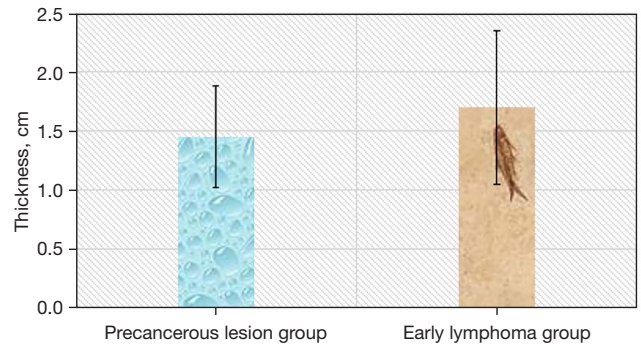


**Figure 4** Comparison of the mean thickness of affected gastric wall between two groups.

commonly involved sites of precancerous lesions were the gastric antrum, followed by the cardia and gastric fundus. There were 21 patients (42.0%) with precancerous lesions and 15 patients (46.9%) with early lymphoma. There was no statistically significant difference in lesion sites between the two groups ( $P>0.05$ ) (Figure 3).

The gastric wall thickness in the early lymphoma group was 0.2–3.1 cm, with an average thickness of  $1.70\pm 0.65$  cm. In the precancerous lesion group, the wall was 0.3–3.1 cm, with an average thickness of  $1.45\pm 0.43$  cm. There was no significant difference in the affected gastric wall thickness between the two groups ( $P>0.05$ ) (Figure 4).

**Comparison of  $\delta 1$  and  $Q1$  of the arterial phase and plain scan CT between the two groups**

The values of  $\delta 1$  and  $Q1$  were compared between groups. The respective mean values of  $\delta 1$  in the early lymphoma and precancerous lesion groups were  $14.57\pm 6.86$  and  $17.28\pm 7.61$  Hounsfield units (HU), the maximum values were 24.00 and 36.88 HU, and the minimum values were 4.00 and 2.72 HU. There was no significant difference in the  $\delta 1$  values between the two groups ( $P>0.05$ ). The respective mean values of  $Q1$  in the early lymphoma and precancerous lesion groups were  $1.30\pm 0.21$  and  $1.40\pm 0.16$ , the maximum values were 1.60 and 2.35, and the minimum values were

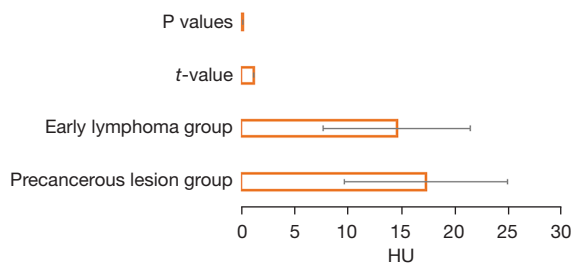


**Figure 5** Comparison of the density difference  $\delta_1$  values of the arterial phase and plain scan CT between the two groups. CT, computed tomography; HU, Hounsfield units.

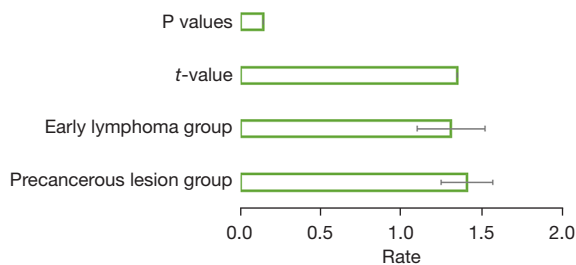


**Figure 6** Comparison of the density ratio  $Q_1$  values of the arterial phase and plain scan CT between the two groups. CT, computed tomography.

1.01 and 1.07. There was no significant difference in  $Q_1$  between groups ( $P > 0.05$ ) (Figures 5,6).

**Comparison of the density difference  $\delta_2$  and ratio  $Q_2$  of the portal phase and plain scan CT between the two groups**

The values of  $\delta_2$  and  $Q_2$  were compared between the two groups. The respective mean values of  $\delta_2$  in the early lymphoma and precancerous lesion groups were  $29.50 \pm 6.05$  and  $41.55 \pm 10.10$  HU, the maximum values were 44.70 and 70.40 HU, and the minimum values were 17.00 and 21.83 HU. There was significant difference between the two groups ( $P < 0.05$ ). The respective mean values of  $Q_2$  in the early lymphoma and precancerous lesion groups were  $1.70 \pm 0.05$  and  $2.06 \pm 0.31$ , the maximum values were 2.12 and 3.02, and the minimum values were 1.33 and 1.46. There was a significant difference in  $Q_2$  between the two groups ( $P < 0.05$ ) (Figures 7,8).

**Calculation of ROC curve**

The AUC value of the maximum area under the ROC curve

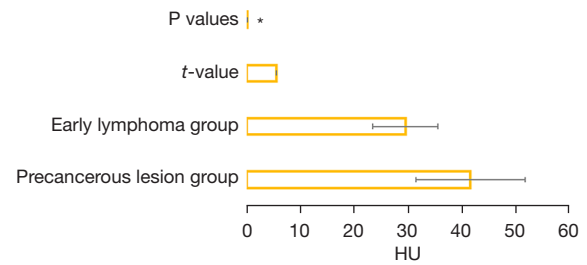


**Figure 7** Comparison of the density difference  $\delta_2$  values of the portal phase and plain scan CT between two groups. \*,  $P < 0.05$ . CT, computed tomography; HU, Hounsfield units.

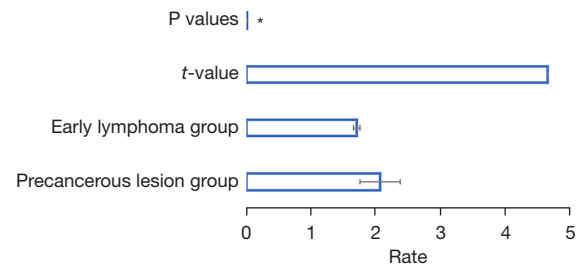


**Figure 8** Comparison of the density ratio  $Q_2$  values of portal phase and plain scan CT between two groups. \*,  $P < 0.05$ . CT, computed tomography.

of early lymphoma and precancerous lesions was 0.755 using the density difference of the portal venous phase and plain scan CT. When  $\delta_2 = 35.63$  HU, the specificity was 89.60%, sensitivity was 67.50%, and the YI was 0.498. According to the density ratio  $Q_2$  of the portal venous phase and plain scan CT, the AUC of the maximum area under the ROC curve of early lymphoma and precancerous lesions was 0.878. When  $Q_2 = 1.86$ , the specificity was 89.60%, sensitivity was 64.90%, and the YI was 0.472. Cases in the two groups that were consistent with  $\delta_2 \geq 35.63$  HU and  $Q_2 \geq 1.86$  were further obtained. After the calculation, the diagnostic specificity of the combination of the two indicators was 98.99% and the sensitivity was 56.80% (Figure 9).

**Discussion**

There is an integral connection between the histological structure of early gastrointestinal lymphoma and precancerous lesions detected by dynamic enhanced CT; that is, precancerous lesions usually occur in the gastrointestinal tract mucosa, muscle fiber and epithelium.

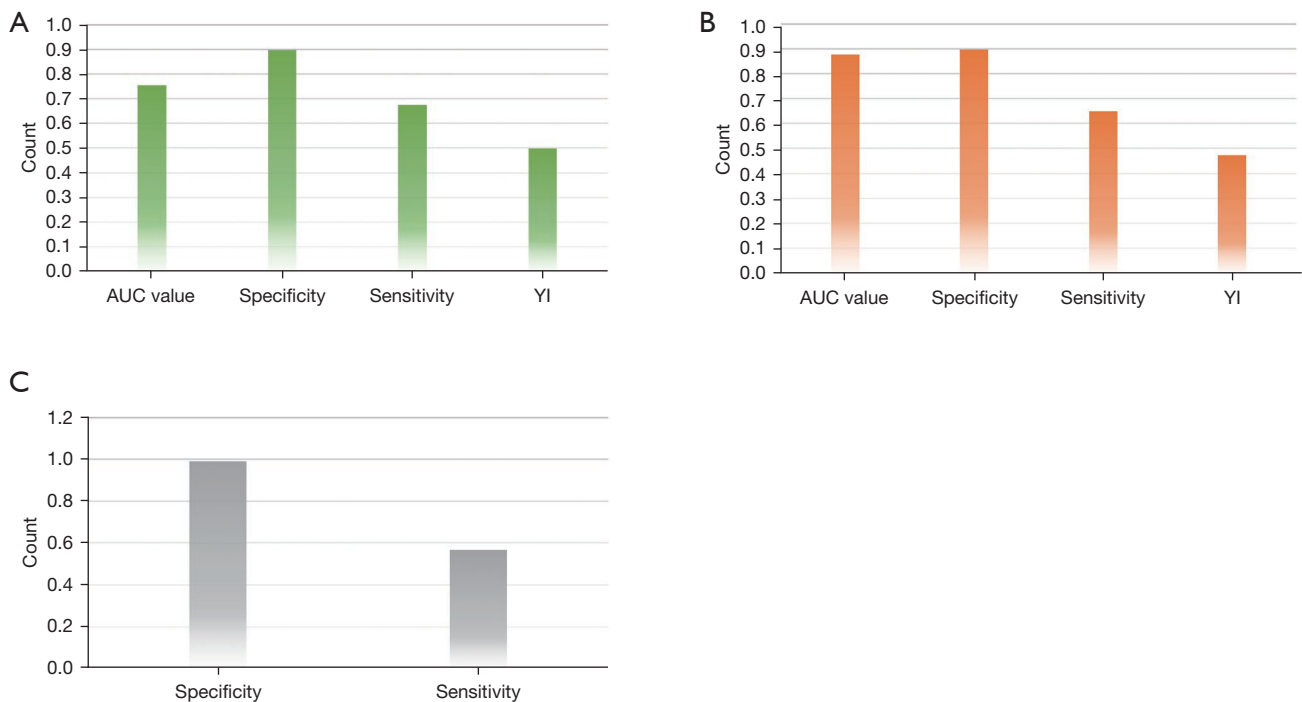


**Figure 9** Calculation results of the ROC curve. Results obtained by the density difference  $\delta 2$  values (A) and by the density ratio  $Q 2$  values (B) of the portal phase and plain scan CT. (C) Result of combining the two indexes. AUC, area under the ROC curve; CT, computed tomography; ROC, receiver operating characteristic; YI, Youden index.

During pathological change, many vascular endothelial growth factors are released, which contribute to neo-angiogenesis. The CT manifestation of contrast agent retention at the venous stage is continuous enhancement (22,23). Lymphoma is a solid tumor originating in the lamina propria of the gastric mucosa and the lymphocytic follicular cells of the submucosa. The dense arrangement of tumor cells leads to poor blood supply, so the degree of enhancement is not as high as in precancerous lesions (24). The significant histological differences in blood supply are reflected in the dynamic enhanced CT images. However, the CT perfusion or dynamic enhanced CT examination is time-consuming, and the corresponding diagnostic images are obtained later from the workstation. So even though both CT perfusion and dynamic enhanced CT examination can provide hemodynamic information for the differential diagnosis of early lymphoma from precancerous lesions, they are not performed widely in the daily practice (25).

Currently, there are few studies related to dynamic enhanced CT for early gastrointestinal lymphoma diagnosis. Ma *et al.* (26) showed that the density difference  $\delta 1$  of the arterial phase and plain scan CT in early gastric

lymphoma and the density difference  $\delta 2$  of the portal phase and plain scan CT were increased by  $\approx 8$  and  $\approx 18$  HU on average, respectively. Moreover, the  $\delta 1$  and  $\delta 2$  of precancerous lesions were increased by 18 and 38 HU on average, respectively. In this study, the values of both are refined, and on this basis, the ratio  $Q$  between arterial phase, portal vein phase and plain CT density is introduced. We used ROC curve analysis to find the optimal threshold for differentiating early lymphoma from precancerous lesions. There was no significant difference between  $\delta 1$  and  $Q 1$  ( $P > 0.05$ ), but a significant difference between  $\delta 2$  and  $Q 2$  ( $P > 0.05$ ), which could be related to the vascular distribution of the two diseases. The blood supply of precancerous lesions is good, but the CT enhancement in the arterial phase is not obvious because most are capillaries. However, obvious enhancement occurred after contrast agent filling in the venous phase or delayed phase. In contrast, the poor blood supply of early-stage lymphoma showed the difference in enhancement mainly in the venous phase.

By analyzing the calculation results of the ROC curves, when  $\delta 2 \geq 35.63$  HU and  $Q 2 \geq 1.86$ , precancerous lesions were more likely to be diagnosed. The specificity was

89.60% and 67.50%, respectively, and the sensitivity was 89.60% and 64.90%, respectively, which indicated that the diagnosis efficiency of  $\delta 2$  was similar to that of  $Q 2$ . However, both had high sensitivity and specificity. Therefore, they can be used as effective indexes to differentiate early lymphoma from precancerous lesions. Further analysis with  $\delta 2$  and  $Q 2$  showed that the diagnostic specificity of the two indexes combined was 98.99%, and the sensitivity was 56.80%. Although the sensitivity decreased, the specificity increased markedly, which indicated that when  $\delta 2 \geq 35.63$  HU and  $Q 2 \geq 1.86$ , dynamic enhanced CT could be used to diagnose precancerous lesions. This conclusion is similar to that of Niu *et al.* (27).

## Conclusions

We explored using dynamic enhanced CT scan for differential diagnosis of early gastrointestinal lymphoma and precancerous lesions. Our results showed that when the two indexes,  $\delta 2$  and  $Q 2$ , were combined, the specificity and sensitivity of diagnosis were 98.99% and 56.80%, respectively. Therefore, dynamic enhanced CT and  $Q 2$  effectively differentiated early gastrointestinal lymphoma from precancerous lesions, and improved diagnostic accuracy. However, the sample in this study was relatively small, so it needs to be expanded in the future clinical trials.

## Acknowledgments

*Funding:* This study was supported by the Huizhou Science and Technology Plan Project (No. 2021WC0106383).

## Footnote

*Reporting Checklist:* The authors have completed the STARD reporting checklist. Available at <https://tcr.amegroups.com/article/view/10.21037/tcr-22-1085/rc>

*Data Sharing Statement:* Available at <https://tcr.amegroups.com/article/view/10.21037/tcr-22-1085/dss>

*Conflicts of Interest:* All authors have completed the ICMJE uniform disclosure form (available at <https://tcr.amegroups.com/article/view/10.21037/tcr-22-1085/coif>). The authors have no conflicts of interest to declare.

*Ethical Statement:* The authors are accountable for all aspects of the work in ensuring that questions related

to the accuracy or integrity of any part of the work are appropriately investigated and resolved. The study was conducted in accordance with the Declaration of Helsinki (as revised in 2013). The study was approved by ethics board of Huizhou Municipal Central People's Hospital (No. kyll20210108) and informed consent was taken from all the patients.

*Open Access Statement:* This is an Open Access article distributed in accordance with the Creative Commons Attribution-NonCommercial-NoDerivs 4.0 International License (CC BY-NC-ND 4.0), which permits the non-commercial replication and distribution of the article with the strict proviso that no changes or edits are made and the original work is properly cited (including links to both the formal publication through the relevant DOI and the license). See: <https://creativecommons.org/licenses/by-nc-nd/4.0/>.

## References

1. Ohmoto A, Fuji S. Histological transformation in malignant lymphoma: a possible role of PET/CT and circulating tumor DNA as noninvasive diagnostic tools. *Expert Rev Hematol* 2020;13:23-30.
2. Jiang M, Bennani NN, Feldman AL. Lymphoma classification update: T-cell lymphomas, Hodgkin lymphomas, and histiocytic/dendritic cell neoplasms. *Expert Rev Hematol* 2017;10:239-49.
3. Buske C, Hutchings M, Ladetto M, et al. ESMO Consensus Conference on malignant lymphoma: general perspectives and recommendations for the clinical management of the elderly patient with malignant lymphoma. *Ann Oncol* 2018;29:544-62.
4. McCarten KM, Nadel HR, Shulkin BL, et al. Imaging for diagnosis, staging and response assessment of Hodgkin lymphoma and non-Hodgkin lymphoma. *Pediatr Radiol* 2019;49:1545-64.
5. Abdelwahed Hussein MR. Non-Hodgkin's lymphoma of the oral cavity and maxillofacial region: a pathologist viewpoint. *Expert Rev Hematol* 2018;11:737-48.
6. Kono Y, Kusumoto C, Kiguchi T, et al. Gastrointestinal: Rapid emergence of double-expressor lymphoma after *Helicobacter pylori* eradication therapy. *J Gastroenterol Hepatol* 2021;36:299.
7. Lane J, Price J, Moore A, et al. Low-grade gastrointestinal lymphoma in dogs: 20 cases (2010 to 2016). *J Small Anim Pract* 2018;59:147-53.
8. Yeo SH, Jung K, Park MI, et al. Mucosa-associated

- Lymphoid Tissue Lymphoma-mimicking Primary Gastrointestinal Small Lymphocytic Lymphoma. *Korean J Gastroenterol* 2020;75:212-5.
9. Saito M, Suzuki H, Kono K, et al. Treatment of lung adenocarcinoma by molecular-targeted therapy and immunotherapy. *Surg Today* 2018;48:1-8.
  10. Mwazha A, Nhlonzi GB, Mazenganya P. Gastrointestinal Tract Plasmablastic Lymphoma in HIV-Infected Adults: A Histopathological Review. *Int J Surg Pathol* 2020;28:735-48.
  11. Lei GY, Tay KV, Teo LT. Rare primary B-cell lymphoma of small intestine presenting as giant jejunal diverticulum and complicated by phytobezoar and intestinal obstruction. *ANZ J Surg* 2021;91:E238-9.
  12. Cheng J, Guo J, North BJ, et al. Functional analysis of deubiquitylating enzymes in tumorigenesis and development. *Biochim Biophys Acta Rev Cancer* 2019;1872:188312.
  13. Zheng C, Jia HY, Liu LY, et al. Molecular fingerprint of precancerous lesions in breast atypical hyperplasia. *J Int Med Res* 2020;48:300060520931616.
  14. Li ZW, Zhou SH. Laryngopharyngeal reflux disease and laryngeal precancerous lesions. *Zhonghua Er Bi Yan Hou Tou Jing Wai Ke Za Zhi* 2017;52:637-9.
  15. Miyazaki T, Shinkawa H, Takemura S, et al. Precancerous Lesions and Liver Atrophy as Risk Factors for Hepatolithiasis-Related Death after Liver Resection for Hepatolithiasis. *Asian Pac J Cancer Prev* 2020;21:3647-54.
  16. Zhang Y, Zhou P. Value of endoscopy application in the management of complications after radical gastrectomy for gastric cancer. *Zhonghua Wei Chang Wai Ke Za Zhi* 2017;20:160-5.
  17. Guo L, Xiao X, Wu C, et al. Real-time automated diagnosis of precancerous lesions and early esophageal squamous cell carcinoma using a deep learning model (with videos). *Gastrointest Endosc* 2020;91:41-51.
  18. Hyodo R, Takehara Y, Nishida A, et al. "Speckled Enhancement" on Gd-EOB-DTPA Enhanced MR Imaging of Primary Hepatic Mucosa-associated Lymphoid Tissue Lymphoma. *Magn Reson Med Sci* 2021. [Epub ahead of print]. doi: 10.2463/mrms.mp.2021-0069.
  19. Ozaki K, Ikeno H, Koneri K, et al. Primary hepatic diffuse large B-cell lymphoma presenting unusual imaging features. *Clin J Gastroenterol* 2020;13:1265-72.
  20. Örgüç S, Arkun R. Tumor-like Lesions of Bone and Soft Tissues and Imaging Tips for Differential Diagnosis. *Semin Musculoskelet Radiol* 2020;24:613-26.
  21. Huynh DK, Toscano L, Phan VA, et al. Ultrathin disposable gastroscope for screening and surveillance of gastroesophageal varices in patients with liver cirrhosis: a prospective comparative study. *Gastrointest Endosc* 2017;85:1212-7.
  22. Bakhshi S, Bhethanabhotla S, Kumar R, et al. Posttreatment PET/CT Rather Than Interim PET/CT Using Deauville Criteria Predicts Outcome in Pediatric Hodgkin Lymphoma: A Prospective Study Comparing PET/CT with Conventional Imaging. *J Nucl Med* 2017;58:577-83.
  23. Liu XH, Jin F, Zhang M, et al. Peripheral T cell lymphoma after chronic lymphocytic inflammation with pontine perivascular enhancement responsive to steroids (CLIPPERS): a case report. *BMC Neurol* 2019;19:266.
  24. Goel Y, Yadav S, Pandey SK, et al. Tumor Decelerating and Chemo-Potentiating Action of Methyl Jasmonate on a T Cell Lymphoma In Vivo: Role of Altered Regulation of Metabolism, Cell Survival, Drug Resistance, and Intratumoral Blood Flow. *Front Oncol* 2021;11:619351.
  25. Zou M, Zhao Z, Zhang B, et al. Pulmonary lesions: correlative study of dynamic triple-phase enhanced CT perfusion imaging with tumor angiogenesis and vascular endothelial growth factor expression. *BMC Med Imaging* 2021;21:158.
  26. Ma Z, Fang M, Huang Y, et al. CT-based radiomics signature for differentiating Borrmann type IV gastric cancer from primary gastric lymphoma. *Eur J Radiol* 2017;91:142-7.
  27. Niu X, Jiang W, Zhang X, et al. Comparison of Contrast-Enhanced Ultrasound and Positron Emission Tomography/Computed Tomography (PET/CT) in Lymphoma. *Med Sci Monit* 2018;24:5558-65.

(English Language Editor: K. Brown)

**Cite this article as:** Chen J, Zhong Y, Zeng X, Huang C, Lan B. Diagnostic test of dynamic computed tomography in early gastrointestinal lymphoma and precancerous lesions. *Transl Cancer Res* 2022;11(6):1689-1696. doi: 10.21037/tcr-22-1085